TAMPEREEN TEKNILLINEN YLIOPISTO
TAMPERE UNIVERSITY OF TECHNOLOGY

ZAHRA KHONSARI

2.4 GHZ INKJET-PRINTED RF POWER HARVESTER ON BULK CARDBOARD SUBSTRATES

Master of Science Thesis

Examiner: Professor Leena Ukkonen
and Professor Lauri Sydänheimo
Examiner and topic approved by the
Council of the Faculty of Computing
and Electrical Engineering on
September 2014

ABSTRACT

TAMPERE UNIVERSITY OF TECHNOLOGY
Master's Degree Programme in Faculty of Computing and Electrical engineering
KHONSARI, ZAHRA: 2.4 GHz Inkjet-printed RF Power Harvester on Bulk Cardboard Substrate
Master of Science Thesis, 50 pages.
August 2014
Major: Radio Frequency Electronics
Examiner: Professor Leena Ukkonen and Professor Lauri Sydänheimo
Keywords: Environmentally friendly electronics, Cardboard substrate, Inkjet printing, Power harvesting, Planar monopole antenna, Battery-less, WiFi.

Inkjet-Printing Technology provides the ability of fabricating electronic circuits on different substrates such as: cardboard, wood, kapton and etc. The advantages of this technology are reduction in production cost in comparison to conventional laminate substrates and also being environmentally-friendly circuits which is one of the main goals in any manufacturing field. Having environmentally-friendly and low cost productions are possible by utilizing paper as the substrate and Inkjet-printing as the fabrication technology.

In addition, reducing the power consumption in any circuit is an important factor in designing a circuit. In any wireless portable device, usage of battery causes a limitation in application space and decreases the lifetime of devices .Since increasing the lifetime of battery is still infeasible, power harvesting energy is one of the solutions in designing battery-less circuits. Power harvesting is a process by which energy is delivered by scavenging DC power from ambient sources. The ambient sources for power harvesting can be light, temperature, motion and electromagnetic in RF (Radio Frequency) range. Among all these sources, ambient RF energy, in both indoor and outdoor is generally available in all hours at different frequency bands. Hence RF energy harvesting is one the most popular type of power harvesting. The ambient RF sources are: Wi-Fi transceivers, AM/FM radio, television broadcasting, mobile networks and communication devices.

In this Project, experimental investigations on the inkjet-printed RF power harvester for 2.4GHz are presented. An one stage discrete rectifier based on a voltage doubler structure and a planar monopole antenna are fabricated on cardboard using inkjet printing. The performance of the whole system is examined by measuring the output voltage of the RF power harvester. By the utilization of the proposed idea, the fabrication of low cost Environmental-friendly battery-less wireless modules is conceivable.

PREFACE

The master thesis, “2.4GHz Inkjet-printed RF Power Harvester on Bulk Cardboard Substrates”, was done in partial fulfilment of the requirement for the Master of Science degree in Radio Frequency Electronics major, in the Department of Electronics and Communications Engineering at Tampere University of Technology. All the researches and investigations have been done in the Wireless Identification and Sensing Systems Research Group (WISE) under the supervision of Prof. Leena Ukkonen and Prof. Lauri Sydänheimo.

I would like to thank my thesis examiners and supervisors, Prof. Leena Ukkonen and Prof. Lauri Sydänheimo for all of their supports, guidance and for providing me an appropriate environment to complete my thesis. I am also thankful to all my colleagues in the WISE Group for their help and support.

Finally, I would like to thank my great parents for all their love, prayers, teaching and motivations through my life.

Tampere, August 2014

Zahra Khonsai

TABLE OF CONTENTS

ABBREVIATIONS

A	Ampere
AR	Axial Ratio
EM	Electromagnetic
E-Plane	A two-dimensional representation of the radiation pattern which contains only electric field and maximum radiation direction.
H-Plane	A two-dimensional representation of the radiation pattern which contains only magnetic field and maximum radiation direction.
cm	Centimeter
dB	decible
DC	Direct Current
DOD	Drop_On_Demand
DPI	Dot Per Inch
EMC	Electromagnetic Compatibility
fL	femto Litre
GHz	Giga Hertz
GND	Ground Plane
HPBW	Half Power Beam Width
Hz	Hertz
MHz	Mega Hertz
mm	Millimetre
nL	nano Litre
pL	pico Litre
Q	Quality factor
RF	Radio Frequency
S	Simens
SOLT	Short-Open-Load-Thru
S-parameters	Scattering parameters
SWR	Standing Wave Ratio
TRL	Through-Reflectin-Line
UV	Ultra Violet
V	Volt
VNA	Vector Network Analyzer
Wb	Weber
wt%	Percent by weight
2D	Two Dimensional
3D	Three Dimensional
µm	micrometre

SYMBOLS

Ω	Ohm
c	speed of light [m/s]
B	Magnetic flux density [wb/m^2]
C	Capacitor per until length [F/m]
D	Electric displacement [C/m^2]
D	Directivity of antenna [dBi]
E	Electric field [V/m]
F	Electric force [N]
G	Conductance per unit length [S/m]
G	Gain of antenna [dBi]
f	frequency [Hz]
H	Magnetic field [A/m]
I(z)	Current wave in z direction [A]
J	Current density [A/m^2]
k	Radiation efficiency of antenna
L	Inductance per unit length [H/m]
L_{RL}	Return Loss [dB]
M	Vector magnetization [A/m]
P	vector polarization [C/m^2]
Q	Electric charge [C]
R	Resistance per unit length [Ω/m]
R_A	Resistance of antenna [Ω]
V(z)	Voltage wave in z direction [V]
W_e	Electric energy [J]
W_m	Magnetic energy [J]
X_A	Reactance of antenna [Ω]
Z_o	Characteristic Impedance [Ω]
Z_A	Impedance of antenna [Ω]
α	Attenuation Constant [NP/m]
β	Propagation Constant [NP/m]
γ	Complex propagation Constant [NP/m]
δ	Skin depth [m]
ε	Permittivity
ε_r	Relative permittivity
ε_0	Permittivity of free space
ε_{eff}	Effective Relative Permittivity
μ	Permeability
μ_r	Relative Permeability
μ_o	Permeability of free space

ρ	Electric charge density [C/m^3]
σ	Conductivity [S/m]
ω	Angular Frequency [rad/s]

1. INTRODUCTION

In any wireless portable device, usage of battery causes a limitation in application space [1] and decreases the lifetime of devices [2-3] .Since increasing the lifetime of battery is still infeasible, power harvesting energy is one of the solutions in designing battery-less circuits. Power harvesting is a process by which energy is delivered by scavenging DC power from ambient sources. The ambient sources for power harvesting can be light, temperature, motion and electromagnetic in RF (Radio Frequency) range [4]. Among all these sources, ambient RF energy in both indoor and outdoor is generally available in all hours at different frequency bands. Hence RF energy harvesting is one the most popular type of power harvesting. The ambient RF sources are: WiFi transceivers, AM/FM radio, television broadcasting, mobile networks and communication devices [2] [4].

Inkjet printing enables additive manufacturing of conductive patterns on a wide variety of platforms based on contactless drop-on-demand deposition of metallic nanoparticle inks. As the material choices in electronic devices have a huge impact on the environment, lately, the use of renewable, environmental-friendly materials, and additive manufacturing methods, such as inkjet-printing, has been a growing trend. Fabrications of electronic circuits are feasible by the inkjet-printing technology on different substrate such as paper [5]. The advantages of implementing circuits on paper are reduction in production cost in comparison to conventional laminate substrates and also being environmentally-friendly circuits. Since paper is suitable for recycling producer [5-6]. In this study, Stora Enso packaging thin cardboard and NPS-JL silver nanoparticle ink are used as substrate and conductor for fabrication of RF electronic circuits, respectively. A Fujifilm Dimatix DMP-2831 material inkjet printer and 10 pL cartridges with 16 nozzles in a single-row arrangement are utilized to print the circuit.

In this Study the results of an experimental investigation on the inkjet-printed power harvester at 2.4 GHz are presented. A passive one-stage discrete rectifier and a planar antenna are fabricated on cardboard using inkjet-printing technology. For the rectifier a voltage doubler structure and for the antenna a planar monopole antenna are utilized. Then, the functionality of the whole module is proven by measuring the output voltage in the real environment. The measurement results demonstrate appropriate absorbed voltage level for feeding a low power circuit by the presented power harvester. By the exploitation of the proposed idea, the fabrication of low-cost environmental- friendly battery-less wireless modules is feasible. Theory and design of Rectifier is explained in Chapter 2. Background theory of electromagnetics and antenna are discussed in chapter 3 and 4, respectively. Chapter 5 deals with introducing the Inkjet-printing technology. Major types of microstrip antennas are explained in Chapter 6 briefly.

Finally, the design procedures, measurement and simulation results of designing antenna and RF energy harvesting are proposed in Chapter 7 and 8. respectively.

2. RF POWER HARVESTER THEORY

Energy harvesting or energy scavenging is a process of converting ambient energy to electrical energy. Due to decreasing the conventional energy sources, finding an alternative renewable energy sources is an important concern. Hence different sources can be a core of Power harvesting such as: solar, thermal, electrostatics, electromagnetics and radio frequency energy. Among of all these kinds of energy, Radio frequency energy harvesting is more attractive because: it is freely available in space, easy to use instead of battery and maintenance the cost. In this case, energy is derived from propagating RF radiation such as cell phones, communication tower, antenna and electronics components [7].

The energy scavenging method can be used in wireless sensor applications, battery-less remote control, mobile phone chargers, RFID and etc [8].

Besides, there are some issues which still need development. Efficiency, output power, output voltage and sensitivity of a RF power harvester requires a considerable study by academic and industry.

Designing the RF power harvesting consists of various steps as is shown in Fig.1. RF power source prepares RF signal, simultaneously rectifier circuit extracts the power and convert it to the DC voltage.

Figure 1. General block diagram of RF Power harvesting.

RF power source: is generally an antenna which RF signal produces a small sinusoidal voltage. The maximum theoretical power is available for RF power harvesting is 0.7 µW and 1.0 µW for 2.4GHz and 900 MHz frequencies, respectively for free space distance of 40 meter.This research is based on GSM-900, in the 930_960 MHz bandwidth and 2.4 GHz.

Impedance matching: the maximum RF power is transferred from source to load by using an input impedance matching circuit. Since the input impedance of the rectifier is different from the RF source (50 Ω), so the impedance matching is needed in case of transferrin maximum power.

Rectifier circuit: Rectifier is able to convert an input RF signal into a considerable DC voltage. Due to low power threshold, the efficiency of rectifier is not high

enough. Hence one of the challenging parts of designing rectifier is having reasonable efficiency.

The output voltage of rectifier is not stable and consists of ripples. Hence, a filter is needed at the output of circuit to have a constant and smooth DC voltage since most of applications need stable voltage.

The load of rectifier could be a resistor, capacitor, inductor or a combination of all these. In this study, a resistive load is used in all simulation and design.

Different parameters are defined to propose a good RF/DC convertor:

- High power conversion efficiency (PCE): efficiency is calculated by:
  $\eta = \frac{P_{out}}{P_{in}}$, $where: p_{out} = \frac{V_{out}^2}{Rload}$
  In order to have the maximum efficiency, the load should be minimum, while higher voltage needs higher resistor. Hence, a tradeoff between high voltage and high efficiency is required.
- Small circuit size: This means having lower number of stage. Designing a circuit with minimum number of stage and capacitor, decreases the size of printed circuit and cost of fabrication.
- Rise time: is defined as the time when the output voltage reaches 90% of the final voltage. Rise time is depending on resistive load and capacitors. The larger rise time causes a delay in the processing of voltage, hence, it is important to reduce the rise time, to reach a stable output voltage in a shorter time.
- Ripple or noise: the voltage which is produced from RF source contains a ripple or noise, which is not desired. This ripple is depending on the current of the load. Hence by using a large capacitor it is possible to smooth the output voltage.
- Voltage conversion efficiency (VCE): is the ratio of the output voltage divided by input RMS voltage.

2.1 RF Power Harvester Variations

As we mentioned before, rectifier has the ability of converting RF power to DC voltage, which is also called as charge pump. It rectifies the input RF signal by using the specific behaviour of diode in rectifying the different level of signal. The simplest rectifier consists of a schottky diode and a parallel capacitor shown in Fig. 2 Voltage doubler is designed in two parts by use of a schottky diode and a capacitor from basic rectifier for performing rectification. The voltage which is stored in input capacitor during negative half of the input cycle is transferred to the output capacitor during positive half of the input cycle. Hence, the voltage at output capacitor is two times of the (peak voltage of RF source - turn on voltage of diode), and because of that it is called voltage doubler. By using voltage doubler in cascade to form the

voltage multiplier the output voltage will increase. In voltage multiplier each stage should add on top of previous stage to receive the DC voltage plus double noise of previous stage [9].

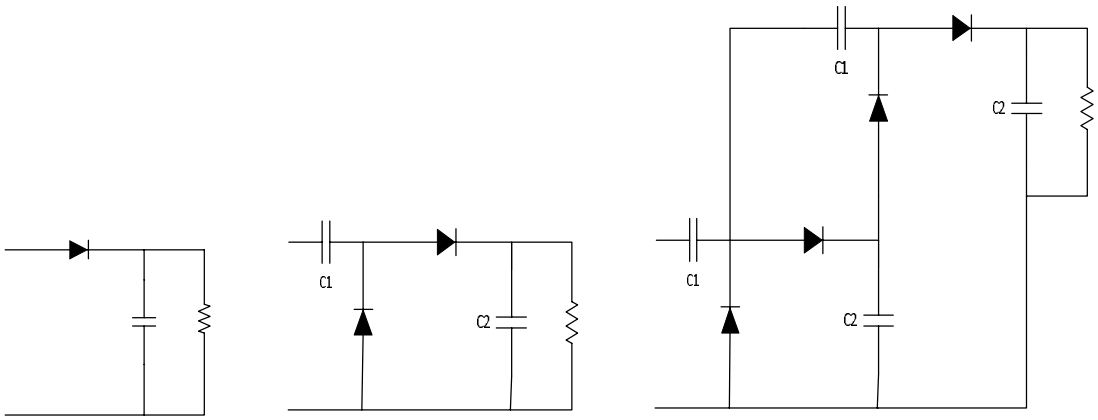

Figure 2. The schematic of basic rectifier, voltage doubler and voltage multiplier.

If, a voltage doubler is seen as a single battery with open circuit output voltage V_o and internal resistance R_0 and Resistive load R_l , then the output voltage is calculated as:

$$V_{out} = \frac{V_o}{R_o + R_l} R_l \qquad (1)$$

When number of stage (n) is increased, the RC values change the time rise of the circuit and also the output voltage alters as:

$$V_{out} = \frac{nV_o}{nR_o + R_l} R_l \qquad (2)$$

Disadvantages of diode based rectifier are limitation in current capacity and regulation. [8]. A summary of comparison between different types of diode based rectifiers is shown in Table. 1.

Table 1. Summry of camparision between diode based rectifier.

type of rectifier	structure	rectifier topology
basic rectifier	A diode connected in series with a load. A capacitor acted as a filter to smoothen the ripple in the output. Commonly called	Half-wave rectifier, full-wave rectifier

	as single-stage rectifier.	
voltage doubler	Uses two stages to approximately double up the DC voltage.	Villard circuit, Greinacher circuit, bridge circuit, Dickson charge pump voltage-doubler
voltage multiplier	Converts RF energy into DC voltage using a network of capacitors and diodes.	Villard cascade voltage multiplier, Dickson multiplier, Cockroft Walton voltage multiplier

As Table.1 shows, diode based rectifiers are designed in different topology base on various applications. Voltage multiplier, not only rectifies RF to DC but also step up the voltage by increasing the number of diode-capacitor stages. Hence for RF energy harvesting application, when higher voltage is needed, the voltage multiplier is one of the best structures.

3. ELECTROMAGNETICS THEORY

Before studying the theory of antenna, it is required to understand electromagnetics theory. By using Maxwell equations properties of electromagnetics wave is defined. Study of electromagnetics theory is started by explaining electric and magnetic fields and representing the concept of plane wave.

3.1 Electric Field

In electrostatics situation when charge is static and there is no time variation field, electric field (V/m) is defined as a force (N) per unit electric charge (C). As equation. 3 shows the electric field depends on the charge and the distance from it.

$$E = \frac{F}{Q} = \frac{Q}{4\pi\varepsilon r^2} r^{\wedge} \tag{3}$$

Where electric fore is calculated as:

$$F = \frac{Q_1 Q_2}{4\pi\varepsilon r^2} r^{\wedge} \tag{4}$$

Where Q_i is electric charge ε is electric permittivity of medium field and r is distance from electric charge. The curl and divergence of electric field is defined as equation. 5 and 6.

$$\nabla . E = \frac{\rho}{\varepsilon} \tag{5}$$

$$\nabla \times E = 0 \tag{6}$$

$$\varepsilon = \varepsilon_0 \varepsilon_r \tag{7}$$

Where ρ is volume charge density (C/m^3), ε_0 is permittivity in free space and ε_r is relative permittivity of medium.

When external field is applied on dielectric body, each atom aligns in the direction of electric field. This phenomenon is called as polarization of dielectric material, which modifies the electric field in/out side of dielectric. Electric flux density or electric displacement D (C/m^2) is defined by equation. 8:

$$D = \varepsilon_0 E + P = \varepsilon E \quad (8)$$

Where P (C/m^2) is vector polarization.

3.2 Magnetic Field

In magnetostatic situation, if time invariant current is available, the magnetic flux density B (Wb/m^2) is described by curl and divergence in equations. 10.

$$\begin{aligned} \nabla \times B &= \mu_0 J \\ \nabla . B &= 0 \end{aligned} \quad (10)$$

Where μ_0 is magnetic permeability and J is current density [12]. If an external magnetic field is supplied in the medium, then moving electric charges experience a force which is calculated by:

$$F = qu \times B \quad (11)$$

Where q is electric charge, u is velocity electricity charge vector. Magnetic polarization in the medium is described in such a way that electric polarization is described. Magnetic intensity H (A/m) is defined as:

$$H = \frac{B}{\mu_0} - M = \frac{B}{\mu} \quad (12)$$

Where M is magnetic vector, and μ permeability of medium [12].

3.3 Maxwell Equations

Maxwell equations are determined by four equations, which defined the relation between electric field, magnetic field, electric charge and electric current in general case. These equations are known as [13]: faraday's law (14), Ampere's critical Law and Gauss's law for electric and magnetic fields.

$$\nabla \times E = -\frac{\partial B}{\partial t} - M \quad (13)$$

$$\nabla \times H = J + \frac{\partial D}{\partial t} \quad (14)$$

$$\nabla . D = \rho \tag{15}$$

$$\nabla . B = 0 \tag{16}$$

In equation. 14, $J = \sigma E$, where σ is the conductivity of material.

3.4 Wave Equations

Maxwell's equations are represented in phasor form, when electric and magnetic fields time dependency is e^{jwt}. for linear, isotropic and homogenous region, maxwell's equation are expressed as [13]:

$$\nabla \times E = -jw\mu H \tag{17}$$

$$\nabla \times H = jw\varepsilon E + \sigma E \tag{18}$$

$$\nabla \times \nabla \times \overline{E} = -j\omega\mu\nabla \times \overline{H} = \omega^2\mu\varepsilon\overline{E} \tag{19}$$

$$\nabla \times \nabla \times A = \nabla(\nabla . A) - \nabla^2 A \tag{20}$$

$$\nabla^2\overline{E} + \omega^2\mu\varepsilon\left(1 - j\frac{\sigma}{\omega\varepsilon}\right)\overline{E} = \nabla(\frac{\rho}{\varepsilon}) \tag{21}$$

$$\nabla^2\overline{H} + \omega^2\mu\varepsilon\left(1 - j\frac{\sigma}{\omega\varepsilon}\right)\overline{H} = 0 \tag{22}$$

$$E(z) = E^+e^{-\gamma z} + E^-e^{\gamma z} \tag{23}$$

$$E(z, t) = Ee^{-\alpha z}\cos(\omega t - \beta z) \tag{24}$$

$$\gamma = \alpha + j\beta = j\omega\sqrt{\mu\varepsilon}\sqrt{a - j\frac{\sigma}{\omega\varepsilon}} \tag{25}$$

3.5 Plane Wave

When E field is in the same direction, same value and same phase in plane perpendicular to the direction of propagation, it is called plane wave (same for H). E and H field have component in transverse plane, which means they are also perpendicular to each other. If plane wave propagate in lossless medium complex propagation is completely imaginary. While if the medium is lossy dielectric then conductivity is zero and the am-

plitude is decrease while wave propagate. For representing the loss of dielectric medium loss tangent ($tan\delta$) is used. Skin depth is utilized for illustrating conductor loss as equation. 26 shows.

$$\delta_s = \frac{1}{\alpha} = \sqrt{\frac{2}{\omega\mu\sigma}} \tag{26}$$

Where w is angular frequency of wave. Hence if the medium is perfect conductor, the EM wave cannot propagate inside [13]. Polarization of EM wave is divided in three types: linear, circular and elliptical. In linear polarization E field vectors vary in one direction, but in circular and elliptical it varies in two dimensions [14]. Axial ratio which defines the quality of polarization varies between 1 and ∞. This for linear polarization it is ∞ and for circular is 1. Fig. 3 shows these different polarizations.

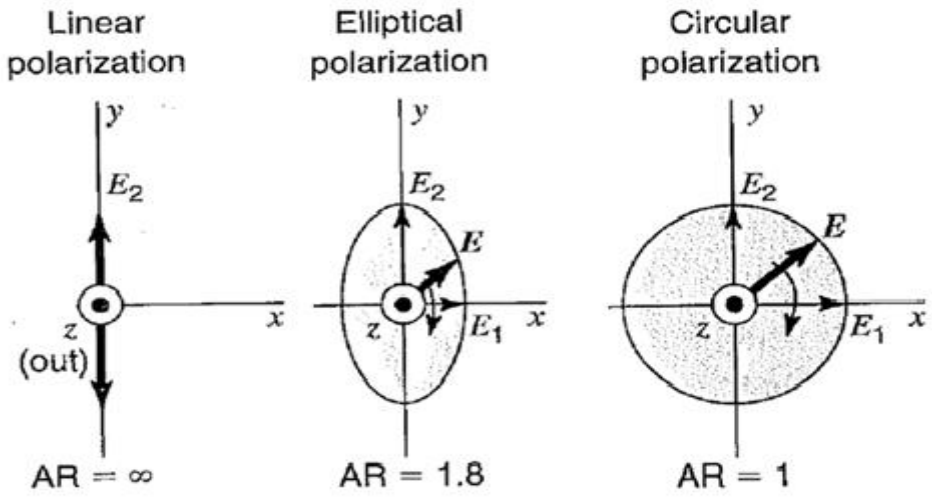

Figure 3. Different polarization types: Linear, Elliptical and Circular polarization [14].

3.6 Energy and Power

In sinusoidal situation, electric and magnetic fields store energy in volume V which are calculated by equations 27 and 28 [13]:

$$W_e = \frac{1}{4} Re \int_V \overline{E}.\overline{D}^* \, dv \tag{27}$$

$$W_m = \frac{1}{4} Re \int_V \overline{H}.\overline{B}^* \, dv \tag{28}$$

The complex power delivered by the source inside the volume V is:

$$P_s = -\frac{1}{2}\int_V \left(\overline{E}.\overline{J}_s^{\,*} + \overline{H}.\overline{M}_s^{\,*}\right) dv \qquad (29)$$

Where $J_s$and M_s are source inside volume V [13].
The complex power flow out of boundary of volume V is calculated as:

$$P_o = \frac{1}{2}\oint_S \overline{E} \times \overline{H}^* ds \qquad (30)$$

Where S is closed surface surrounds volume V. the power dissipated inside volum V is expressed by:

$$P_l = \frac{\sigma}{2}\int_V |\overline{E}|^2 dv + \frac{\omega}{2}\int_V (Im(\varepsilon)\left|\overline{E}\right|^2 + Im(\mu)\left|\overline{H}\right|^2) dv \qquad (31)$$

Poyning's theorem is defined by using above equations.

$$P_s = P_o + P_l + 2j\omega(W_m + W_e) \qquad (32)$$

That says the power delivered by the sources inside volume V is equal to the summation of power dissipated inside the volume V, power transmitted through the boundaries and the 2w times of reactive energy stored in electric and magnetic fields inside the volume [13].

3.7 Transmission Line

In transmission line theory the elements of circuit are distributed in along the line. Fig. 4 shows, the equivalent circuit of lumped element for a very short length of circuit. By using circuit theory voltage and current of this circuit are defined.

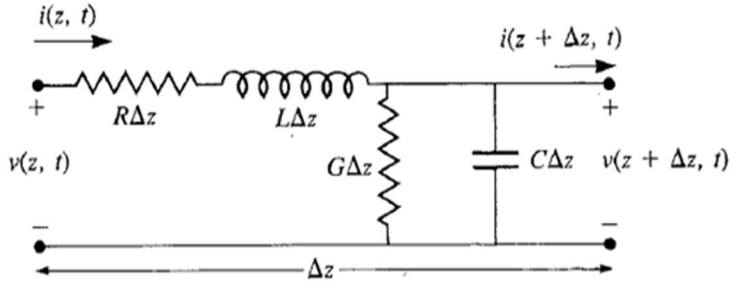

Figure 4. The equivalent circuit for short segment transmission line [13].

The general solutions of two wave equations are determined by voltage and current of transmission line as:

$$V(Z) = V_0^+ e^{-\gamma z} + V_0^- e^{\gamma z} \qquad (33)$$

$$I(Z) = I_0^+ e^{-\gamma z} + I_0^- e^{\gamma z} \quad (34)$$

Where $\gamma = \alpha + j\beta = \sqrt{(R + jwL)(G + jwC)}$ is complex propagation constant, α is attenuation constant, R is series resistance, L is series inductor per length, G is shunt conductance per length and C is shunt capacitance per length. The characteristic impedance of line is described by:

$$Z_o = \frac{V_o^+}{I_0^+} = \sqrt{\frac{(R + jwL)}{(G + jwC)}} \quad (35)$$

By terminating the transmission line in load side, the wave reflection is happened in load part. The voltage reflection coefficient is defined as equation 36 [13]:

$$\Gamma = \frac{V_o^-}{V_o^+} = \frac{Z_L - Z_0}{Z_L - Z_o} \quad (36)$$

The superposition of the incident wave and reflected one make a standing wave along the transmission line which is terminated to a mismatch load ($Z_L \neq Z_o$). The other parameter which can be used to describe the reflection is standing wave ratio (SWR) explained by equation. 37:

$$SWR = \frac{V_{max}}{V_{min}} = \frac{1 + |\Gamma|}{1 - |\Gamma|} \quad (37)$$

3.8 Scattering Parameters

Operation of a network is explained by network port parameters such as: Z-parameters, Y- parameters and ABCD and S-parameters, which describe the relation between input and output port of the network [13]. When frequency is increased, it is not possible to use Z, Y or ABCD parameters. Since these parameters are related to voltage and current, while measuring voltage and current is not feasible with voltmeter and ampere meter. Hence scattering parameter is used in higher frequency. Scattering parameter is calculated as:

$$S_{ij} = \frac{V_i^-}{V_j^+}, when\ V_k = 0\ for\ k \neq j \quad (38)$$

Where i and j are the incidence for the pot of network. Scattering parameter also can be defined by power parameters as equation. 39 shows:

$$S_{ij} = \frac{b_i}{a_j} \text{ , } when\ a_k = 0\ for\ k \neq j \quad (39)$$

Where b_i is reflected power from port i and a_j is reflected power from port j [13].

3.9 Microstrip Line

Microstrip line is a planar transmission line. Fig.5 shows the geometry of conventional microstrip line, where thickness and relative permittivity of substrate are d and ε_r respectively. W is the width of microstrip line.

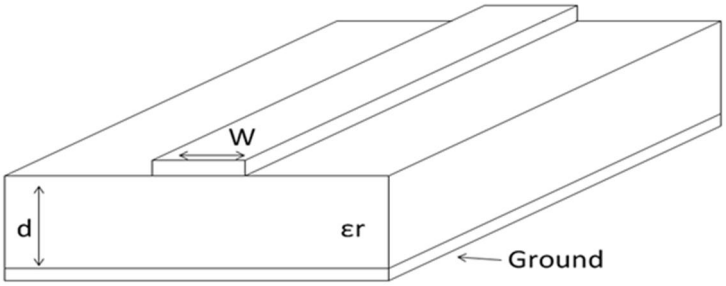

Figure 5. Microstrip's geometry.

Equivalent permittivity of microstrip is a combination of air and substrate [13], because part of fields propagates inside the substrate and the other part propagates in the air. Equivalent permittivity of microstrip line is calculated as equation (40):

$$\varepsilon_{reff} = \frac{\varepsilon_r + 1}{2} + \frac{\varepsilon_r - 1}{2} \frac{1}{\sqrt{1 + 12\frac{d}{W}}} \quad (40)$$

4. BASIC THEORY OF ANTENNA

Antenna is a passive component which starts to radiate when a signal is captured by its port. Different parameters define antenna which are explained here first. The most important parameters are: radiation pattern, half power beam width (HPBW), directivity, gain, input impedance, return loss, bandwidth, polarization and axial ratio.

Moreover antenna is divided in various models, such as: wire antenna, patch antenna, reflector antenna and lens antenna which have different performance applications [15].

4.1 How an Antenna Radiates

Realizing how an antenna radiates is helpful in understanding parameters of antenna. Speed of electric charge in a time-variant current distribution in the antenna structure, produces time-variant *E* and *H* fields around the antenna which propagate in all directions [14]. The space around antenna is divided in 3 regions: reactive near field, radiating near field and far field [15]. In the far-field region the propagated radio wave can be assumed as plane wave.

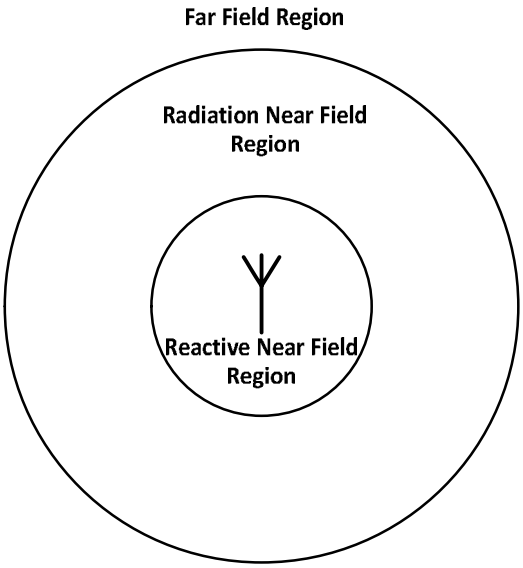

Figure 6. Antenna Feild Regions

Figure. 6 indicates, antenna regions. In far or Fraunhofer region, the field pattern is independent of distance while, in near or Fresnel region the shape of field pattern relates to distance.

4.2 Antennas Parameters

Following explain different parameters of antenna which should be consider in designing an antenna and comparison of different antennas.

4.2.1 Radiation Pattern

Radiation pattern of antenna defines the radiated power by antenna as a function of direction from antenna, which has a 3D dimensional pattern. E plane and H plane illustrate the radiation pattern, where E plane consist of E field vector and H plane consist of H field vector [15].

4.2.2 Half Power Beam Width (HPBW)

Radiation pattern of antenna are three-dimensional quantities consist of the variation of field or power as a function of spherical coordinates θ and φ.

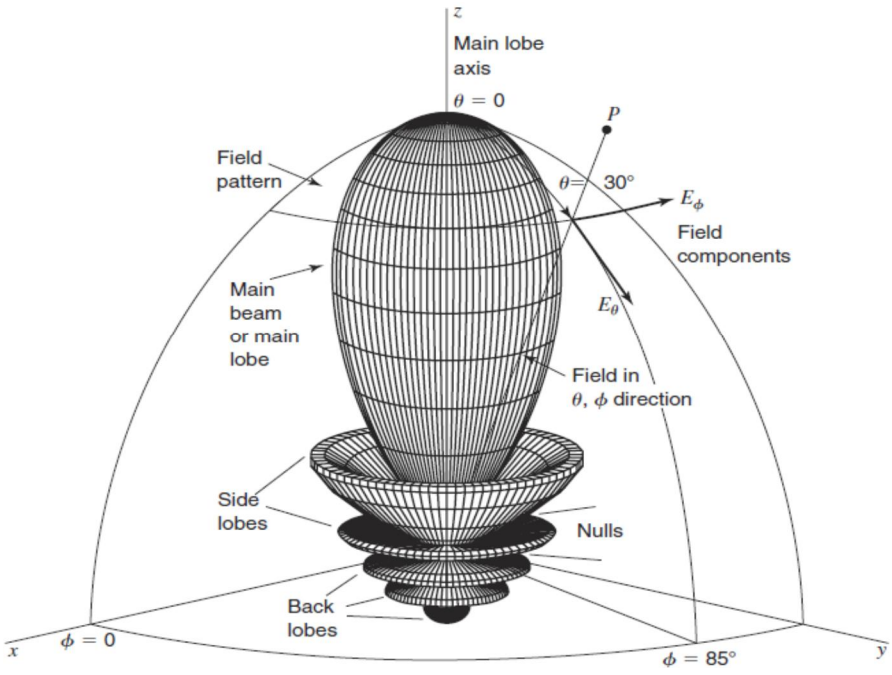

Figure 7. General radiation pattern with its different sections [16].

Figure.7 shows each part of radiation pattern [16] of antenna which is divided in main lobe, side lobe, back lobe, minor lobe and nulls. The angle between the two directions in which the radiation intensity is one-half value of the beam.is called HPBW.

4.2.3 Directivity and Gain

Directivity of antenna is the ratio of maximum power to the average power of antenna.

$$D = \frac{P_{max}}{P_{av}} \tag{41}$$

Gain of antenna depends on directivity and efficiency of antenna(k) as equations show:

$$G = kD \tag{42}$$

$$k = \frac{P_{rad}}{P_{in}} = \frac{P_{rad}}{P_{rad} + P_{loss}} \tag{43}$$

Where $Prad$ is the radiated power by the antenna and $Ploss$ is the power dissipation by ohmic loss of the antenna. Usually the gain of antenna is described as a ratio of gain of the antenna over gain of an isotropic antenna in logarithmic scale. As equations. 44 and 45 show [14]:

$$G(dBi) = 10\log\left(\frac{G}{G_{iso}}\right) = 10\log(G) \tag{44}$$

$$G(dBd) = 10\log\left(\frac{G}{G_{dipole}}\right) = 10\log(\frac{G}{1.64}) \tag{45}$$

4.2.4 Input Impedance and Return Loss

The impedance seen from the antenna port is the impedance of antenna. The real part of impedance demonstrates the loos and radiation of antenna and imaginary part illustrates the energy stored in near-field of antenna [16].

$$Z_A = R_A + jX_A = (R_{rad} + R_{loss}) + jX_A \tag{46}$$

Return loss represent the reflection of the signal when transmission line is terminated to the load or device. Due to the mismatch and decreasing the delivered power to the load, reflection is happened. Thus, its behavior can be modeled as a loss phenomenon. The concept of return loss can be demonstrated using equation. 47 [13].

$$L_{RL}(dB) = -20\log(\Gamma_{in}) \tag{47}$$

4.2.5 Bandwidth

The frequency range which antenna works properly is called bandwidth of antenna. Generally 10 dB return loss is required to define the performance of antenna in frequency spectrum. Hence the return loss of antenna is higher than 10 dB in whole frequency band [15].

4.2.6 Polarization and Axial Ratio

Polarization of antenna is defined as polarization of EM wave. Which can be linear or circular depends on the application of antenna. Axial ratio describes the quality of polarization [14].

5. INK-JET PRINTING TECHNOLOGY

Inkjet-printing is a technology for fabricating printed circuit. This technology provides fast, simple and low-cost production on any substrate. In every implementation of a circuit, fabrication process which affects the cost, reliability and performance is the most important parameters. Various methods are used in fabrication process such as photolithography and direct printing. But direct printing is desired, due to low-cost mass production. The required temperature tolerance of the usage substrate in inkjet-printing technology is lower than conventional printed circuit manufacture. Hence this property makes Inkjet-printing technology suitable for environmentally friendly cardboard, wood and flexible substrates.

Direct writing is divided in four categories: droplet-based DW, energy beam-based DW, flow-based DW and tip-based DW methods.

Droplet-based method consists of two groups: inkjet and aerosol. Inkjet technology is one of the most popular methods which are used as drop on demand (DOD) [17]. The droplet method is based on piezoelectric, thermal, electrostatic or acoustic elements [18]. The general piezoelectric print head is shown in Fig. 8. By applying a voltage pulses to the piezoelectric crystal, the inkjet-printed head is controlled. This pulses cause physical deformation and allow droplet to be spouted. The diameter of each droplet is defined by several parameters, such as: ink, temperature, ink viscosity, jetting voltage and frequency, surface property and surface temperature.

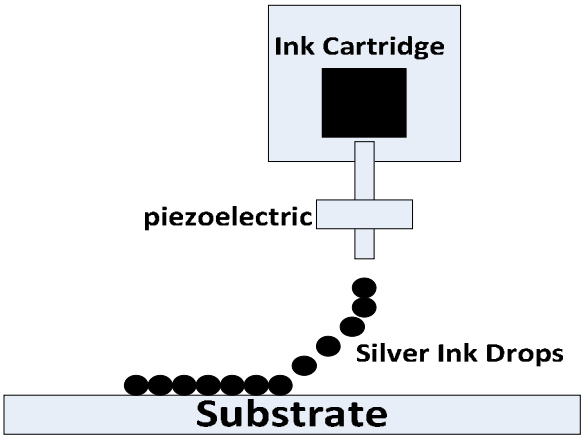

Figure 8. the block diagram of piezoelectric DOD Inkjet-printing technology.

Figure 9. Dimatix DMP 2831 material inkjet printer and The cartridge and head used for printing.

The Diamatix printer (DMP2831), the cartridge and head which are used in this project are shown in Fig. 9.

Sintering is required after printing to form the dielectric solid or conductive trace. In this study thermal sintering method is used. In this method the substrate with printed pattern are placed in conventional oven. Inert atmosphere, formed nitrogen and hydrogen are applied to avoid oxidization. The temperature of oven is set based on the type of ink which is used in printing. For instance for the NPS-JL silver Nanopaste 120ºC/150ºC is sufficient as in [19] is recommended. In general longer time and higher temperature for sintering provides better conductivity. But higher temperature also affects the substrate, since some substrate cannot tolerate higher temperature than 200ºC.

5.1 Characterization of the Substrate and Conductor Ink

Silver ink (NPS-JL silver ink with 55.5wt% metal content) is used in this study as a conductor because of its special properties in comparison with other conductors such as: copper and gold. Silver ink has higher conductivity in compare with copper and reasonable price in compare with gold. Besides, cardboard is used as a substrate. Properties of the cardboard and electrical features of printed conductive ink on cardboard were characterizes in previous study [20], which are used in this thesis.

As the first step for characterization of printed silver ink on cardboard, the appropriate resolution for the printed pattern should be investigated. The most suitable spacing between the droplets is equal to the radius of droplets on the substrate. Which avoid of spreading ink on substrate, also helps to have a good connection between droplets. The radius of droplets depends on properties of ink and substrate such as viscosity, contact angle, temperature, hydrophilicity and roughness. One way for measuring radius of droplets is droplet test.

As mentioned in [20] the best way to print is printing and sintering 2 layers in one turn and printing 8 layers, to have suitable conductivity in proper time. In addition it is better to use an ink-proof dielectric material.to increase the roughness of the surface. Due to by having high roughness, the frequency losses is increased. A conventional primer composed of tetrahydrofurfuryl acrylate, ethoxylated trimethylolpropanetriacry-

late, 2-hydroxy-2-methyl-1-phenyl-propan-1-one,and bis-phenylphosphineoxide is used in the rough and fibrous side of cardboard since the other side has better situation.

Table 2. Properties of Cardboard and printed conductor.

Measured Parameters	Value
Relative Permittivity of cardboard	1.78
Loss tangent of cardboard	0.02
Thickness of cardboard	560µm
Conductivity of silver ink	$2 \times 10^7\ S/m$
Thickness of silver ink	3 µm

5 layers of primer are printed separately with 1061 dpi resolution. After each printing the sample is cured with ultra-violet (UV) light for 10 minutes. Then maintained at 150 ^{o}C for 1 hour in oven. UV light is utilized to improve the printed primer while oven is used to volatilize the water content inside primer ink and avoid the later reaction between primer and silver ink. Table. 2 shows the final results of characterization of card board and printed silver ink.

6. MICROSTRIP ANTENNAS

In this chapter we will study basic and important parameters and performance of microstrip antennas.

Microstrips antennas have gained lots of attention in recent years, due to simplicity of design and fabrications. A microstrip antenna is a small metallic patch, which can be copper, silver or gold on top of a dielectric substrate [21]. The ground of antenna can be on top or under part of antenna depend on requirement of design. Patch antenna, circular antenna, monopole antenna, dipole antenna and array antenna, are types of microstrips antenna which are used in main applications [22].

The advantages of using microstrip antenna are: light weigh, easily integrated with different type of microwave circuits, low cost and low volume [23]. Low cost fabrication is one of main reason, why they are gaining more attention in compare to other type of antennas. Microstrip antenna also has this ability to give linear and circular polarization easily. Moreover feed line can be print at the same time, when fabricating matching or other part of circuit is done.

Besides of all advantages of microstrip antenna, there are some limitations in usage of this type of antenna, such as: narrow bandwidth, low power gain, low efficiency and it is hard to get a fine polarized antenna. But there are several techniques which help to improve these disadvantages. The substrate of antenna has an important affect in performance of antenna, if the substrate is thicker, then the radiated power and impedance bandwidth will be increase and conduction losses is decreased. If the substrate thickness exceeds $0.11\boldsymbol{\lambda}$ then the antenna will stop resonating because of inductive reactance feeding line. Another parameter which also has an effect on antenna performance is dielectric constant ϵ_r . decreasing the dielectric has the same effect as when thickness is increased.

6.1 Major Types of Microstrip Antennas

Depending on geometry, microstrp antennas are divided in many shapes [23]. Properties and similarities of some major categories of microstrip antenna are presented in this chapter.

6.1.1 Microstrip Patch Antennas

The most famous type of microstrip antennas is patch antennas [23]. For the applications which need simple design, patch antennas are one of the best choices. The typical microstrip patch antenna is shown in Fig. 10. These types of patch antenna are useful in

designing dual frequency, linear and circular polarization, Omni directionality, broad bandwidth, beam scanning and etc.

The metallic part of patch antenna is on top of the substrate and the ground part is under substrate. Radiated power of antenna is increased by increasing the thickness of substrate and decreasing the dielectric constant of substrate. Impedance matching can be done by feeding line to the patch which holds a large number of charges. The repulsive force between negative and positive charge, force to the charges to move towards edges, which are a source or radiations.

The shape of microstrip patch antennas can be: rectangular, circular, triangular and elliptical. Resonance frequency relates to length of patch antenna, but width of it, does not have much effect on resonance frequency than the radiated power, bandwidth and radiation efficiency.

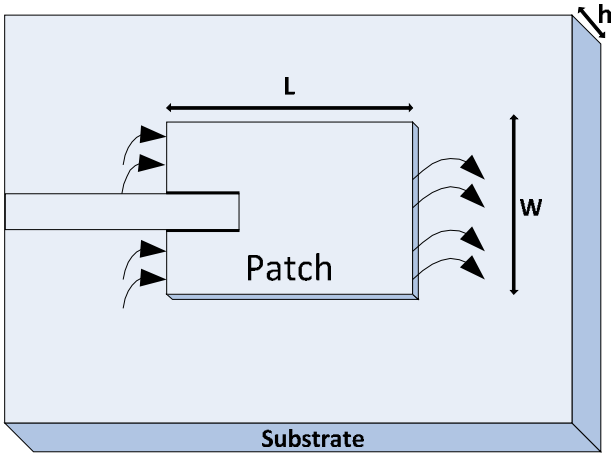

Figure 10. Typical Microstrip patch antenna [24].

6.1.2 Microstrip Dipole Antennas

Microstrip dipole antenna becomes popular recently, since they can design in smaller size, with good linear polarization and suitable for wireless equipment [25]. This type of antenna, have been in many different design for various applications such as: dual band, omni-directionality. Feeding port of dipole has a great effect on performance of dipole depends on the position of it. In addition ground plane can be under the dipole structure or under the radiating part. The general dipole antenna is presented in Fig. 11.

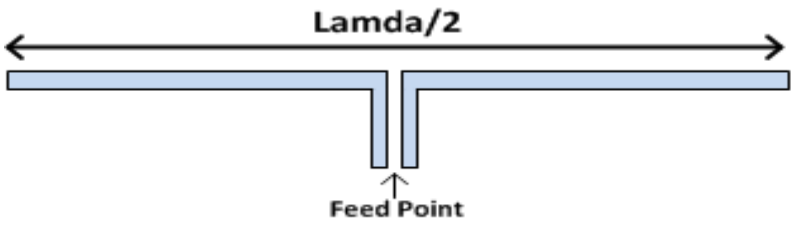

Figure 11. Typical Dipole antenna.

6.1.3 Microstrip Slot Antennas

Microstrip slot antennas have a slot in the ground plane [26]. It can be fed through a microstrip line or through a coplanar waveguide, like patch antenna. This type of antenna can have bi/uni directional radiation pattern, with wider bandwidth [27].

6.1.4 Microstrip Travelling-wave Antennas

Microstrip travelling wave antenna (Fig. 12) can be in various shapes such as: long thin microstrip line or continues repeating chain shaped structure with the matched load attached to the other end of it. This matched load, avoids the standing waves on the antenna. Radiation beam of this antenna can be set to any direction, with the help of some design techniques.

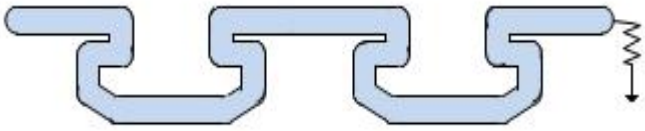

Figure 12. Model of Travelling wave antenna [28].

6.1.5 Planar Monopole Antenna

A monopole antenna generally is a vertical wire which is mounted on a ground plane (Fig.13). Bandwidth of monopole antenna is changed by variable diameter of antenna. A planar monopole antenna is a cylindrical monopole antenna with large effective diameter [29]. It also can be as a Metamaterials Surface Antenna (MSA) on a thin substrate which can has a large BW.

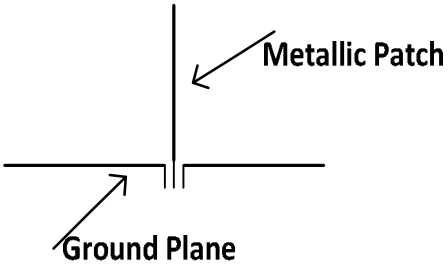

Figure 13. General Planar Monopole Antenna.

Planar monopole antenna can be in various shapes depends on application as Fig.14 shows: square, rectangular, triangular, hexagonal, circular and elliptical.

Figure 14. Various model of planar monopole antenna [29].

A planar rectangular monopole antenna is chosen in this study as basic geometry to design the final antenna. The explanation brings the main properties and design producer of the planar rectangular monopole antenna.

For a planar monopole antenna a lower frequency and physical dimension for VSWR=2 are approximately calculated from below equations [29]. Assume that the rectangular planar is equivalent to cylindrical monopole antenna with same height L and radius r.

$$2\pi rL = WL \tag{48}$$

$$r = W/2\pi \tag{49}$$

$$f_L = \frac{7.2}{L + r + p} GHz \tag{50}$$

Where p is probe length and all parameters are in centimeter.

The input impedance of a $\boldsymbol{\lambda}/4$ monopole antenna is half of $\boldsymbol{\lambda}/2$ dipole antenna. The BW of this antenna is mainly depends on length of probe (p), diameter of feeding probe (d) and width of plate (W). When SMA connector is used for feeding the antenna parameter d is remain constant at 0.12 cm [29]. If L is increase then the lower edge frequency decrease.

As inkjet printing is possible for implementing planar monopole antenna, microstrip antenna is one of the best choices for printing on cardboard as substrate. In addition the antenna which is chosen in this case should be unbalanced since the RF power harvester circuit is unbalanced. The input impedance of antenna is 50Ω, due to the whole system is in 50Ω impedance. Since we need an antenna for WiFi band, so having a wideband antenna is not required.

7. DESIGN PROCEDURE

In this chapter, design procedure of printing rectifier and antenna by using ink-jet printing technology is explained.

7.1 Design Procedure of Rectifier at 950 MHz

Fig. 15 shows the steps of designing RF power harvester, which consists of designing: antenna, matching circuit and voltage doubler. First of all we start from designing the voltage doubler and then go to other steps.

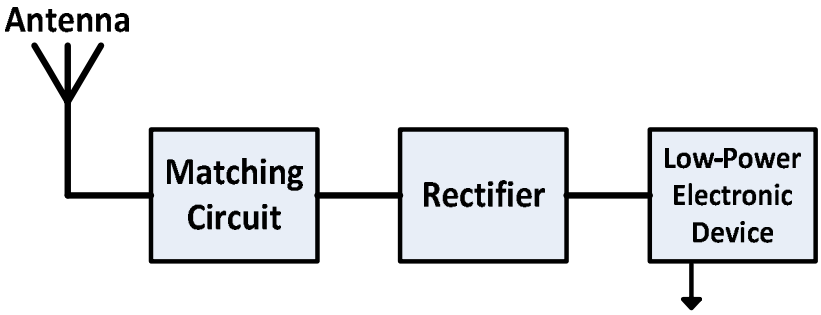

Figure 15. General block diagram of RF energy harvesting system.

In this study, a voltage doubler is designed by using 2 zero bias schottky surface amount HSMS-2850 [10], which is designed to use in the presence of a small signal (Pin < -20 dBm) and at frequencies below 1.5 GHz. In addition, it provides a low forward voltage, low substrate leakage, high switching speed and uses symmetric properties of a diode that allows unidirectional flow of current under ideal condition [10]. Hence, if the input voltage is higher than the diode forward voltage then the circuit can be practicable.

The specific parameters of diode are given by Agilent in data sheet. These parameters, listed in Table. 3 are used in Advance Design System (ADS) software to model the diode by its equivalent circuit.

Table 3. The electrical parameters of schottky diode [10].

Parameters	Units	HSMS-2850
B_V	V	3.8
C_{j0}	pF	0.18
E_G	eV	0.69
I_{BV}	A	3 E-4

I_S	A	3 E-6
N		1.06
R_S	Ω	25
$P_B(V_J)$	V	0.35
P_T(XTI)		2
M		0.5

If the effect of diode substrate is neglected, then the diode is model as Fig. 16 Where C_j is junction capacitance, R_j is junction resistance.

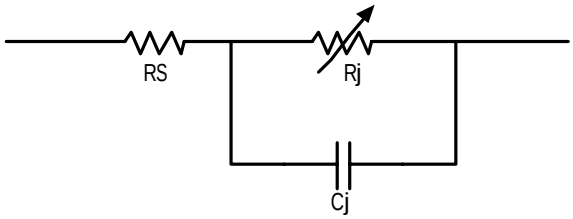

Figure 16. The equivalent circuit of the schottky diode used in ADS.

Simulation and practical implementation is done at 950 MHz ± 50 MHz, which is closed to the center frequency of GSM-900 transmitter. The simulation is also performed using the same schematic depicted in Fig. 4, with C1 and C2 equal to 1nF and 1µF, respectively. 10K ohm is chosen as optimum load, due to by increasing the load resistance the output voltage also increased but the output power will decrease, Hence a trade-off is needed in this case. The circuit used in this study can be seen in Fig.17. The circuit is simulated in ADS using large signal S-parameter method. After simulation the circuit is then printed on a cardboard with silver ink by Fujifilm Dimatix DMP-2831 material inkjet printer. The printing is done in 4 steps and in each step, two layers is printed in order to achieve a better conductivity.

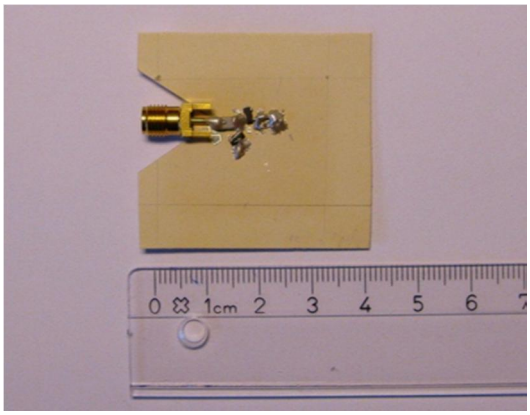

Figure 17. The fabricated rectifier using inkjet printing technology on cardboard.

The output voltage of RF-conversion without matching circuit is shown in (table. 4 and Fig. 18)

Table 4. Comparision of experimental and simulation results.

Input power (dBm)	Output voltage / Measurement (mV)	Output voltage / Simulation (mV)
10	3020	2560
5	1621	1322
0	825	634
-5	392	268
-10	172	88
-15	68.09	20
-20	24.1	12
-25	8	0.356

From the Fig. 18, it can be seen that measurement and simulation are approximately agree with each other. The measurement results are shown to be better than simulation. The reason may be related to the resistance value of diode which may be lower than the simulation model [9]. In this case the DC voltage at 10dBm in simulation and measurement are 2.568 V and 3.02 V respectively.

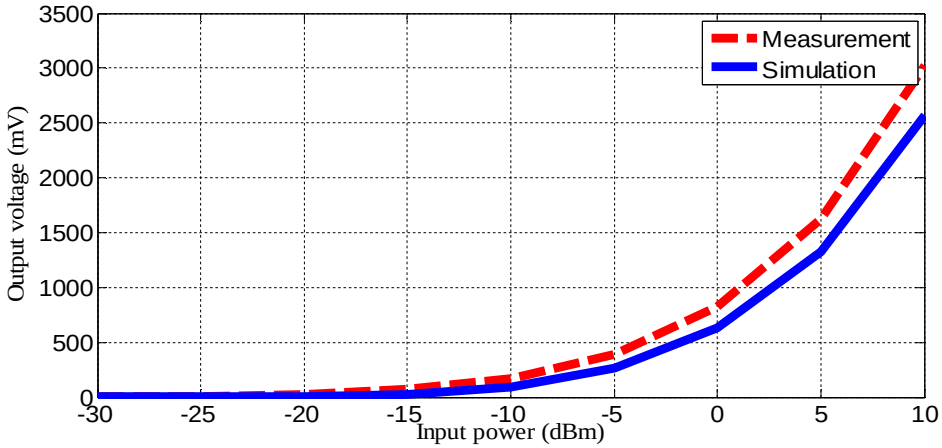

Figure 18. **The simulation and measurement results for the output voltage of the rectifier versus the input power.**

In the next step, the input impedance of the printed circuit is measured by Vector Network Analyzer (VNA) and then the matching part is added to the circuit in order to transfer the maximum available power from antenna to rectifier. The complete schematic of RF power harvester is shown in Fig. 19.

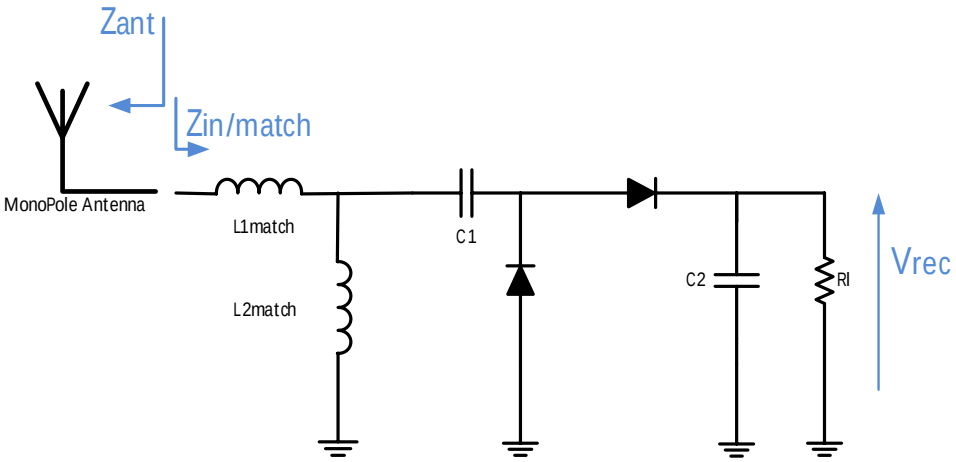

Figure 19. The matching circuit block diagram.

The fabricated rectifier with impedance matching circuit is shown in Fig. 20. Different power levels (dBm) by the aim of " hp ESG-D3000A Signal Generator" are applied as input power of rectifier to investigate the input reflection coefficient of rectifier.

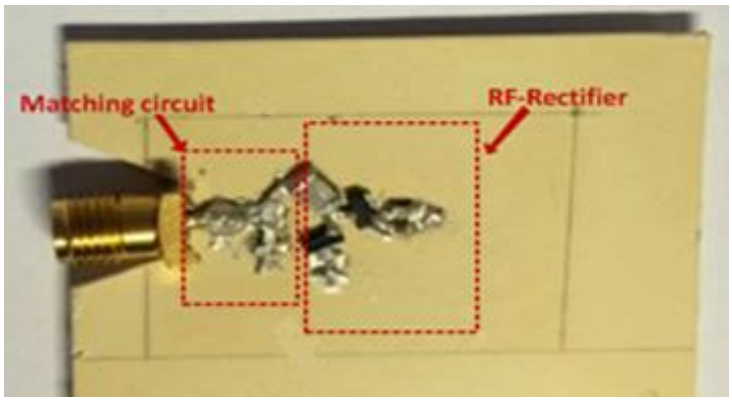

Figure 20. The fabricated rectifier with impedance matching circuiusing inkjet printing technology on cardboard.

Fig. 21 shows the return loss (S11) at 950 MHz frequency, which performs similar to the simulation result. The circuit is perfectly matched in desired frequency for different input power levels.

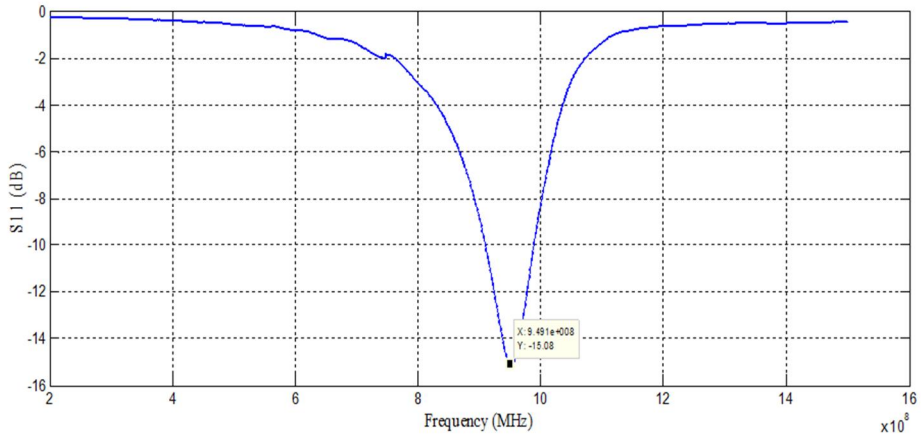

Figure 21. Input reflection coefficient result of rectifier after adding matching circuit.

The output voltage is measured by using digital signal generator @950MHz for various input power. The output voltage is increased after adding the matching part in compare to previous result. For instance the output voltage for 0dBm input power before matching was 1.6V, while it reaches to 2.1 V after adding the matching circuit.

From the Fig. 22, it can be seen that measurement and simulation are approximately agree with each other. The measurement results are shown to be better than simulation. The reason may be related to the resistance value of diode which may be lower than the simulation model [9].

Table 5. Comparision of experimental and simulation results after adding matching circuit.

Input power (dBm)	Output voltage / Measurement (mV)	Output voltage / Simulation (mV)
10	5150	3011
5	3530	1600
0	2100	1040
-5	1160	865
-10	601	365
-15	296.46	197
-20	129.77	78
-25	52.46	61

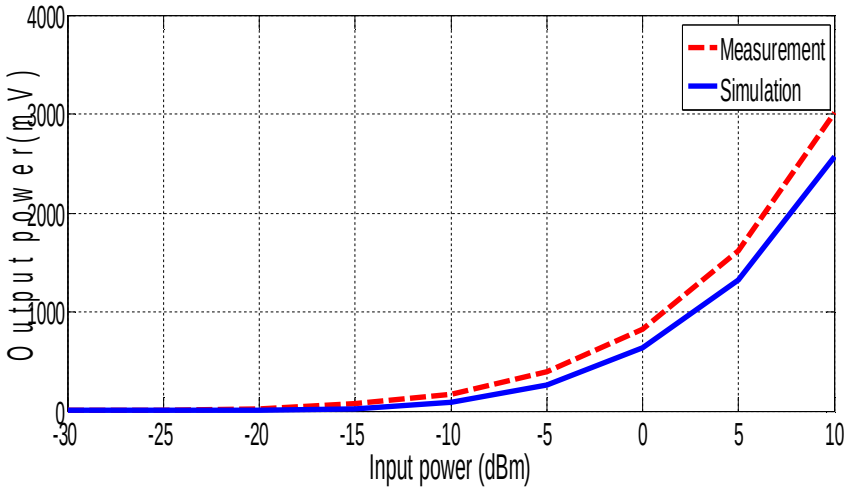

Figure 22. The simulation and measurement results for the output voltage of the rectifier versus the input power.

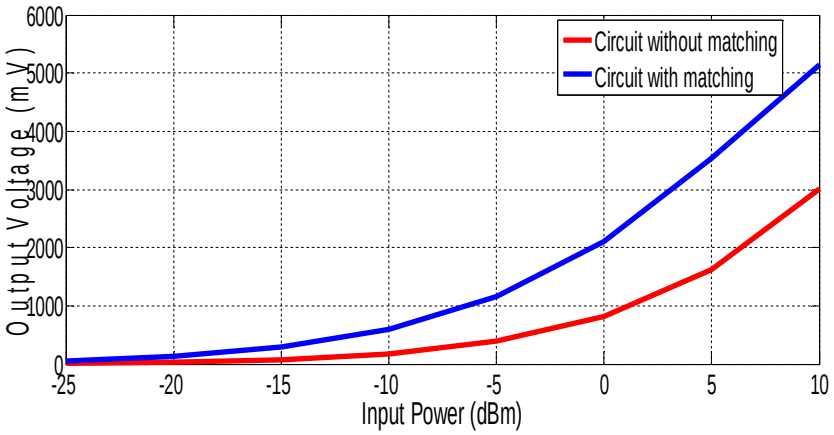

Figure 23. comparision of output voltage before/after adding matching circuit.

From fig.23, it can be seen that the output voltage is increased after adding the matching circuit as expected.

7.2 Design Procedure of Rectifier at 2.4 GHz

Same steps are done as previous part to design the rectifier @ 2.4GHz. In this case, it was assumed that the input power is more than -20 dBm. Hence, HSMS 28020 zero surface shcottky diode [11] is chosen for fabricating the circuit. Which is suitable for >-20 dBm input power up to 4GHz. Table. 6 shows the Pspice, model of diode.

Table 6. Electrical parameters of schottky diode [11].

Parameters	Units	HSMS-2850
B_V	V	1.5
C_{j0}	pF	0.7
E_G	eV	0.69
I_{BV}	A	1 E-4
I_S	A	2.2 E-6
N	-	1.068
R_S	Ω	6.0
$P_B(V_J)$	V	0.65
P_T(XTI)	-	2
M	-	0.5

First of all, a single HSMS 2820 Diode is placed on cardboard with the silver ink trace to investigate the input impedance of diode. From the Fig. 24, it can be seen that the input power changes slightly for specific input power range.

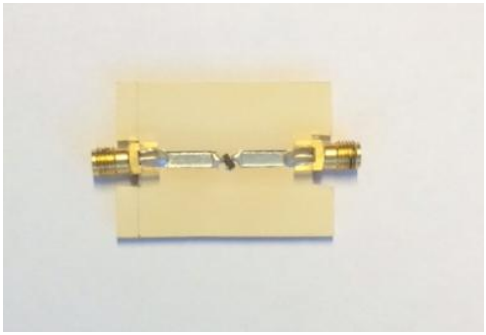

Figure 24. Prototype for measuring input impedance of HSMS 2820

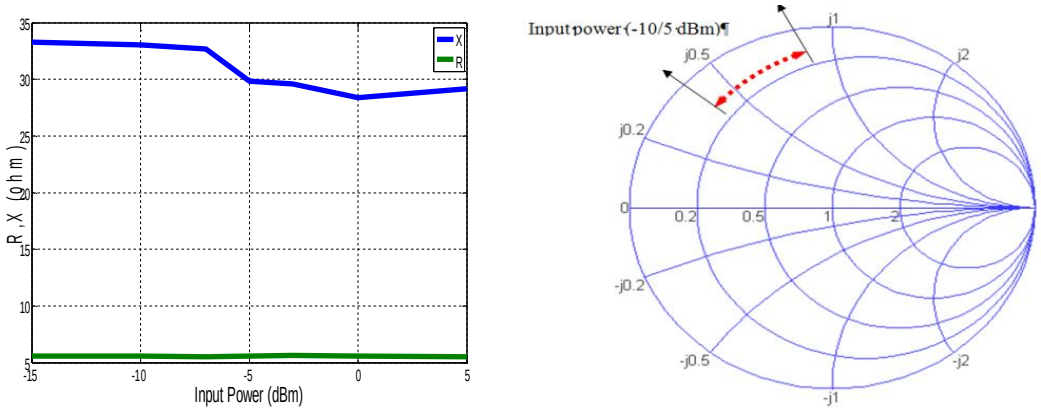

Figure 25. Measyrment result of input impedance of HSMS-2820 Zero surface schcottky diode.

Then, the rectifier was fabricated @ 2.4GHz to measure the input impedance of by VNA and then the matching circuit was added to matched the input impedance of rectifier in all input power range (-10 to 5 dBm). Fig. 26 shows the fabricated rectifier with/without matching circuit.

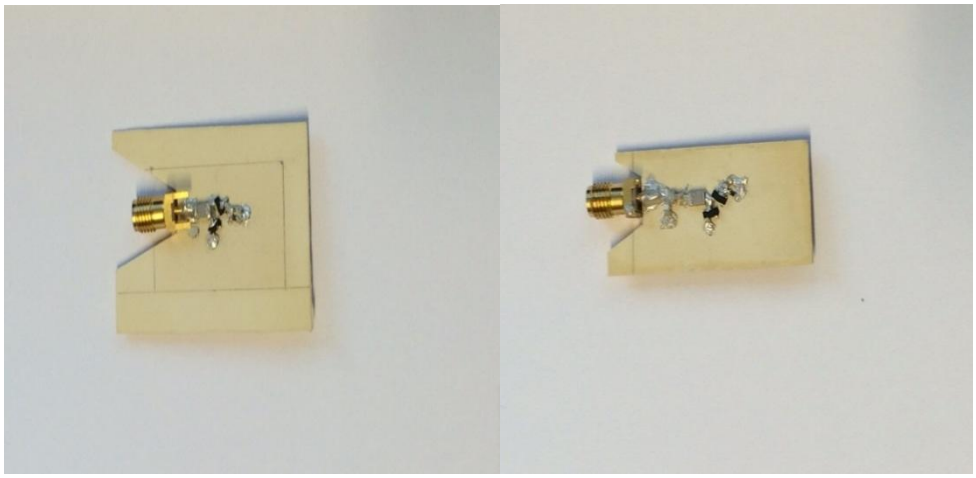

Figure 26. Fabricated Voltage doubler on Cardboard with/without matching circuit.

A series capacitor and a shunt inductor were used in matching network as shown in Fig. 27.

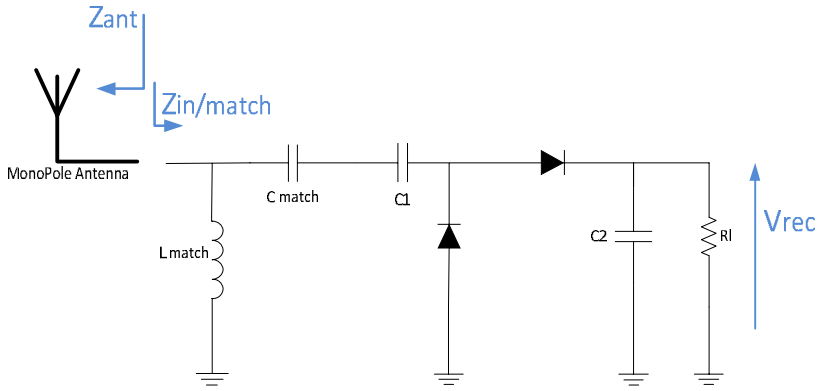

Figure 27. schematic of added matching network to rectifier.

Fig. 28 shows the input return loss (dB) of rectifier for various input power. The circuit is perfectly matched from (-5 to 5 dBm) and it goes to -7dB for -10 dBm input power.

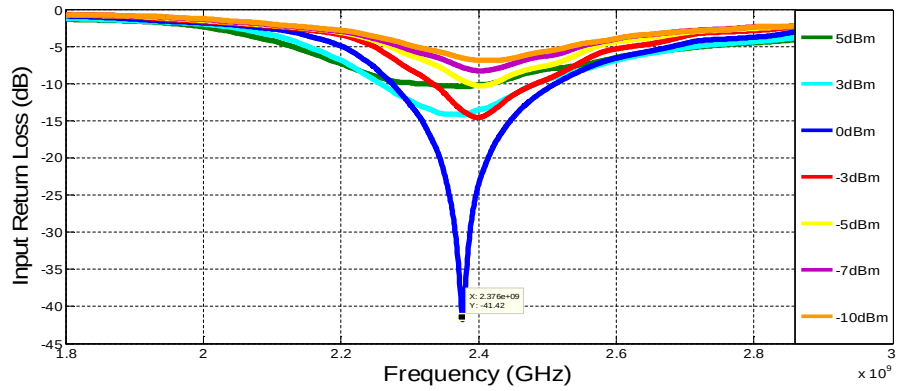

Figure 28. The input return loss versus different input power level.

The output voltage was measured for both circuits by Signal Generator @ 2.4GHz. Fig.29 presents that the output voltage for instance @ 0dBm is almost 1.2V after adding the matching circuit.

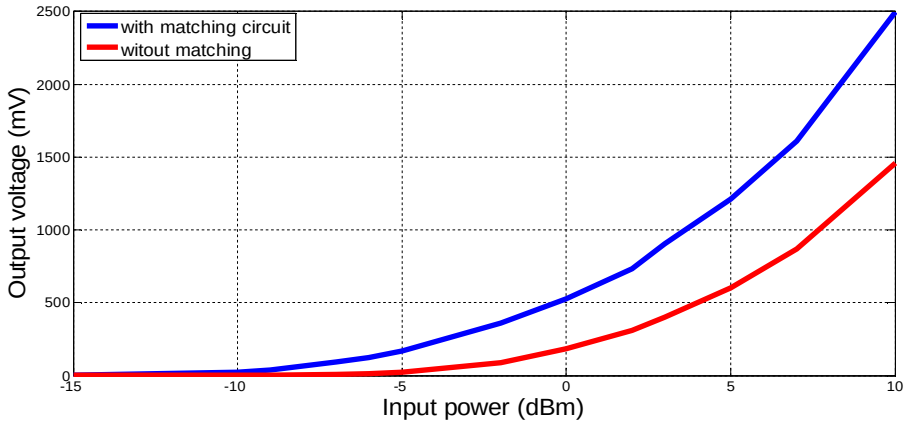

Figure 29. The measurment output voltage versuse various input power levels.

7.3 Design Procedure of Planar Monopole Antenna

A planar monopole antenna can be considered as a patch antenna if the ground plane is infinity [30]. Due to the majority of space compare to thin substrate is air, hence air can be assumed as substrate. The geometry of rectangular monopole antenna is depicted in Fig. 30.

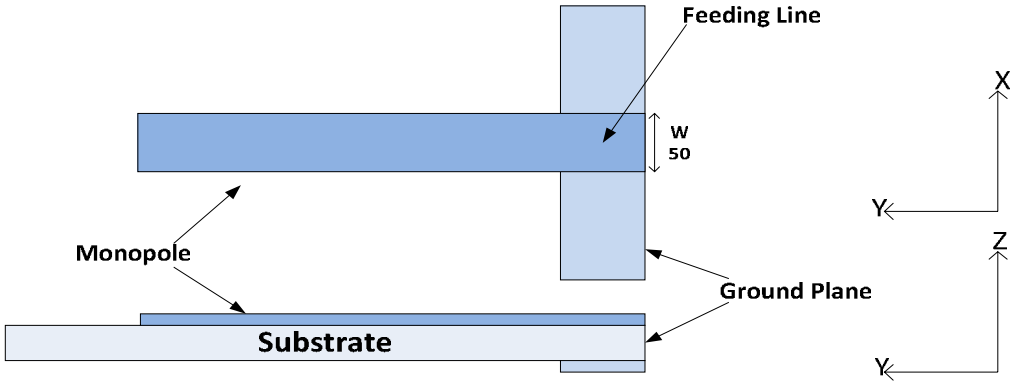

Figure 30. Geometry of general planar monopole antenna.

For decreasing the size of antenna, several parameters (Wa=Width of antenna, La= length of antenna, Wg= width of ground and Lg= length of ground) are tuned. Also bending the antenna helps to reduce the height of final antenna. Fig. 31 proposed the final geometry of planar monopole antenna.

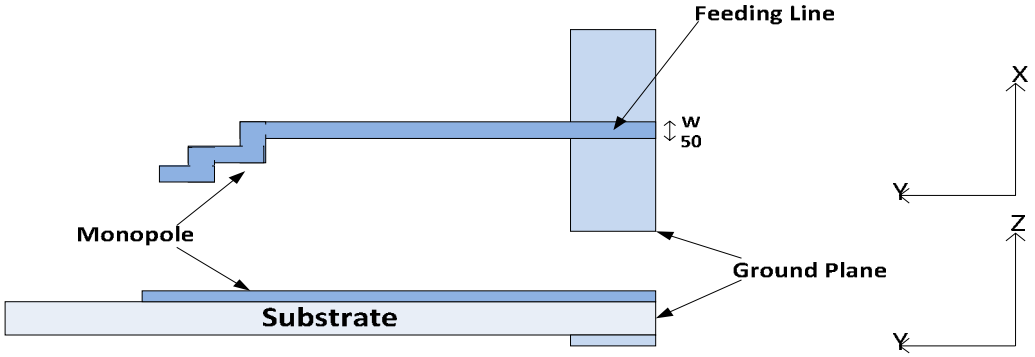

Figure 31. Geometry of proposed antenna.

Figures (32-34) shows the ultimate results of simulation in desired frequency (2.4GHz).The summery of physical dimensions of proposed planar monopole antenna is presents in Table. 7.

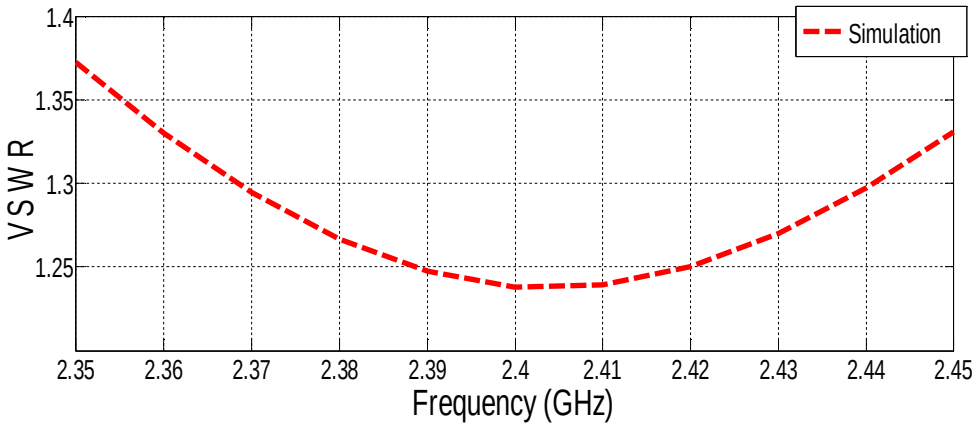

Figure 32. VSWR or Impedance BW simulation plot of antenna.

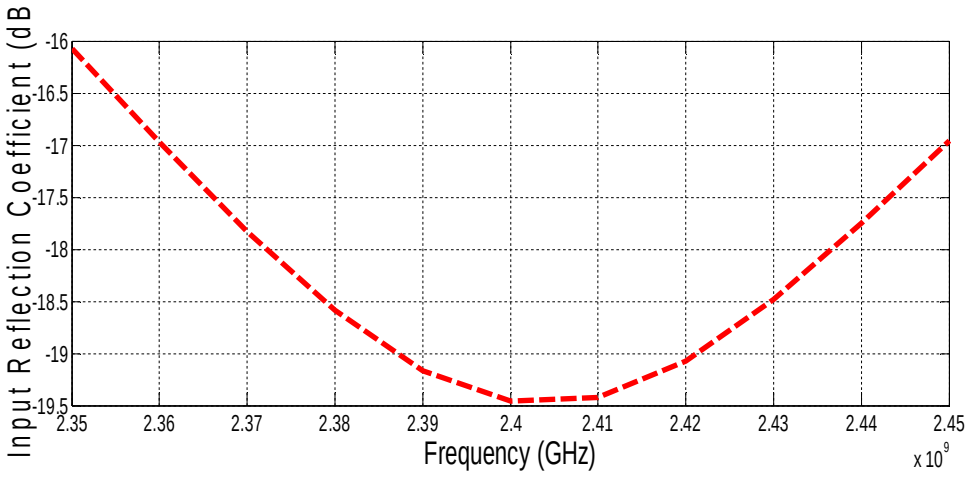

Figure 33. The simulation of the input matching of proposed antenna rectangular planar monopole antenna.

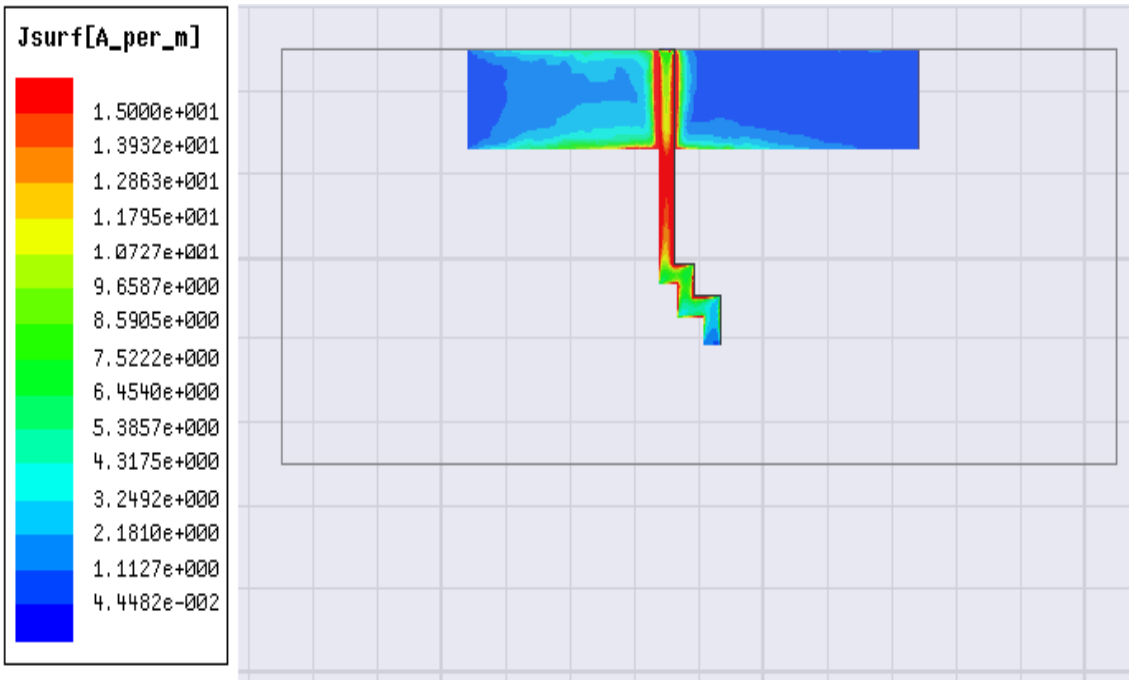

Figure 34. The current distribution of in the proposed antenna structure at 2.4GHz.

Table 7. The summery of the physical dimensions of proposed planar monopole antenna.

Physical parameter	Length (mm)
La	35
W50	2.5
Lg	12
Wg	70

7.4 Simulation and Measurement Results

According to the final results of simulation, the proposed antenna is printed on cardboard with the aim of surface treatment. Fig. 35 presents the fabricated inkjet-printed planar monopole antenna.

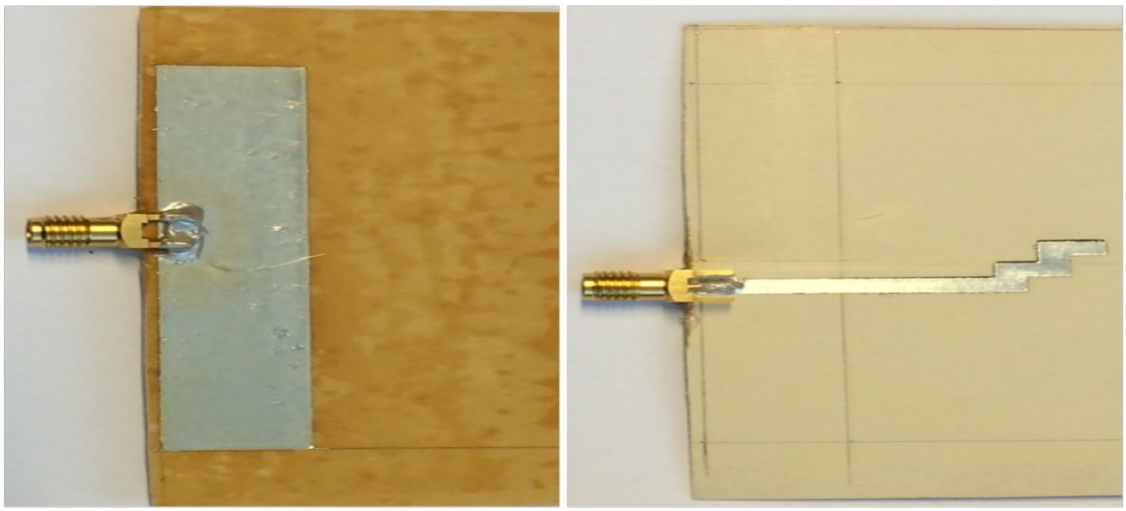

Figure 35. The inkjet-printed planar monopole antenna on cardboard. Top and Bottom sides.

The simulation and measurement results of input reflection coefficient of proposed antenna (S_{11}) is depicted in Fig. 36. The results are in a good agreement with simulation however, the measurement is not perfectly accurate due to the effect of other instruments in measurement environment. Besides, during the printing monopole antenna the width of it is increased a bit due to displacement of layers during printing procedure. As simulation shows, it is expected by increasing the width, center frequency is shifted to lower.

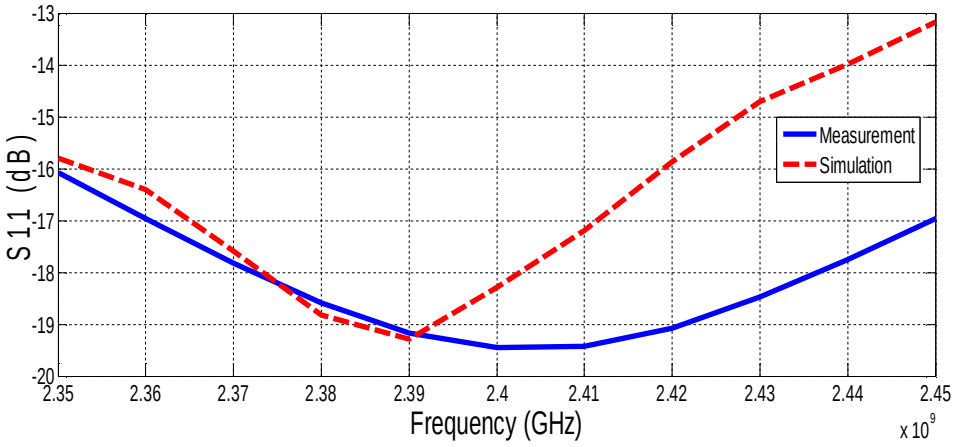

Figure 36. The simulation and measurment result of Input return loss of proposed antenna.

Fig. 36 shows the simulation and experimental results of efficiency of antenna in desired frequency range.

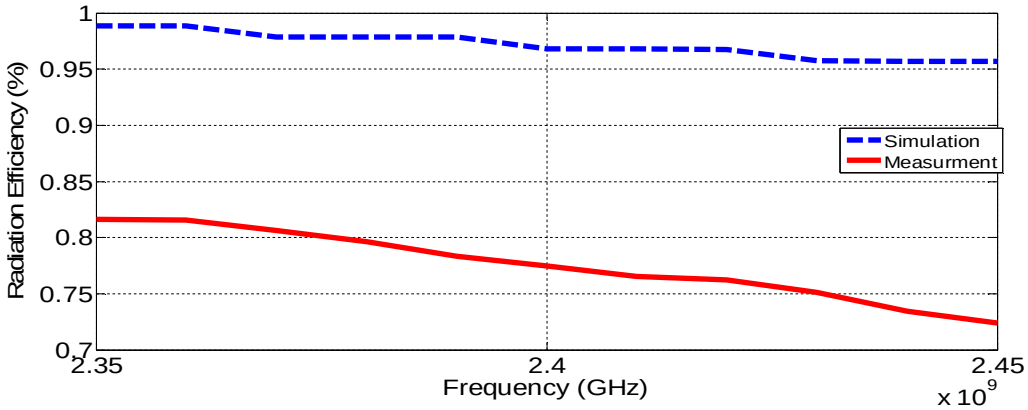

Figure 37. The simulation and measurment result of radiation efficiency of proposed antenna.

Experimental result of maximum gain is illustrated in Fig. 38 which is also measured in Satmio Star Lab for desired frequency range. the maximum gain of proposed antenna is 2.7 dB which is enough good result for printed antenna on cardboard.

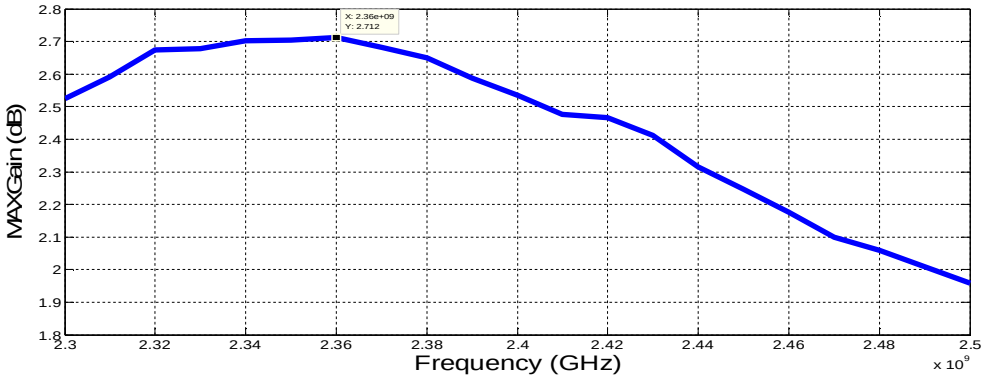

Figure 38. The measurment result of maximum realized gain of proposed antenna.

Other parameters which need to be investigated are radiation patterns of antenna. The simulation and measurement result of E-plane and H-plane at 2.4GHz are demonstrated

in Fig. 39 and Fig. 40. The H-plane is Omni-directional in desired frequency range. E-plane is like an ordinary radiation pattern of monopole antenna

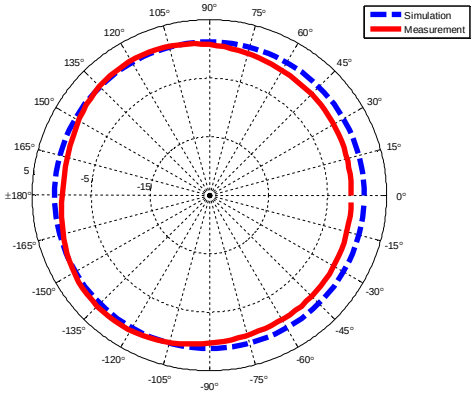

The measured and simulation radiation of antenna in H-Plane

Figure 39. The measured and simulation radiation pattern of proposed antenna in H-Plane.

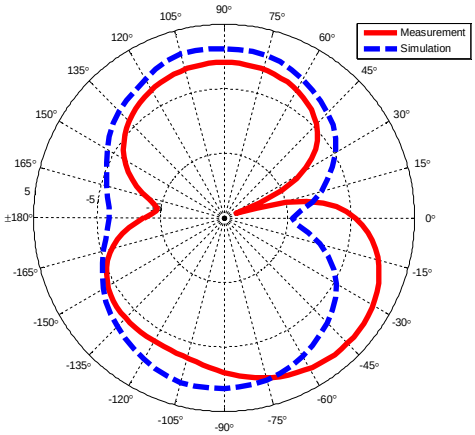

The measured and simulation radiation pattern of antenna in E-Plane

Figure 40. The simlation and radiation pattern of proposed antenna in E-Plane

Measurement and simulation results of 3D radiation pattern of proposed antenna are presented in Fig.41. As it can be seen, results are in a good agreement.

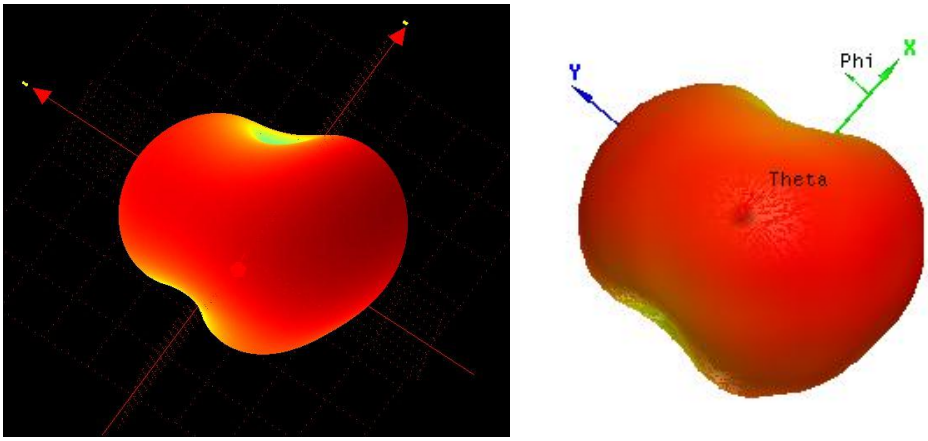

Figure 41. 3D Measurement and Simulation of Radiation Pattern of Proposed Antenna

8. RESULTS OF ENERGY HARVESTING SYSTEM

RF harvesting system which is consist of a rectifier and a planar monoploe antenna is illustretaed in Fig. 42.

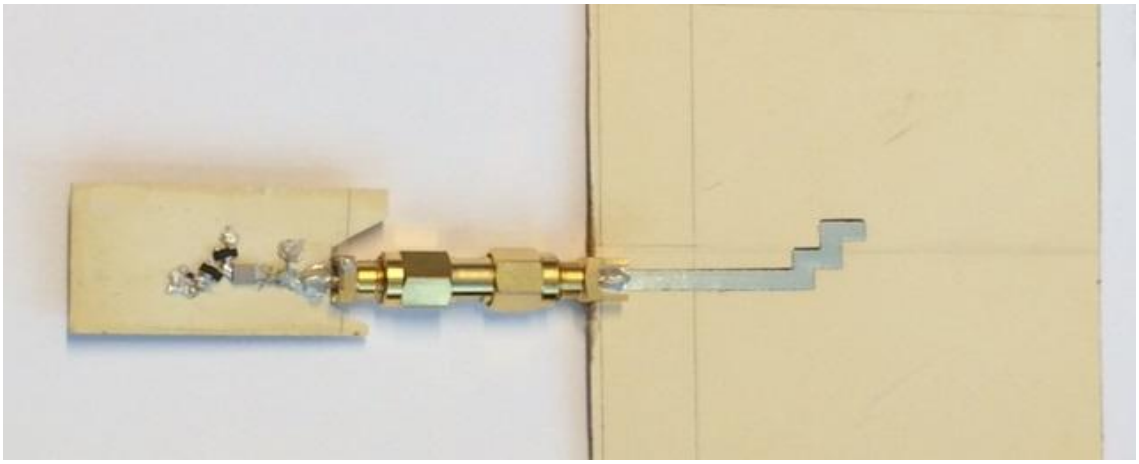

Figure 42. The fabricated RF energy Harvester fat 2.4GHz.

For investigating the performance of the system, a patch antenna [30] as is shown in Fig.43, which was designed for 2.4 GHz is used as transmitter to power the antenna of rectifier. Fig. 44 indicates the gain and efficiency of patch antenna.

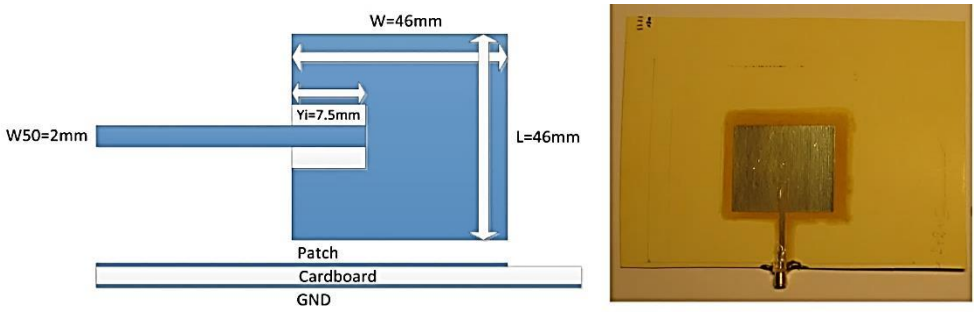

Figure 43. The fabricated Patch antenna as power source.

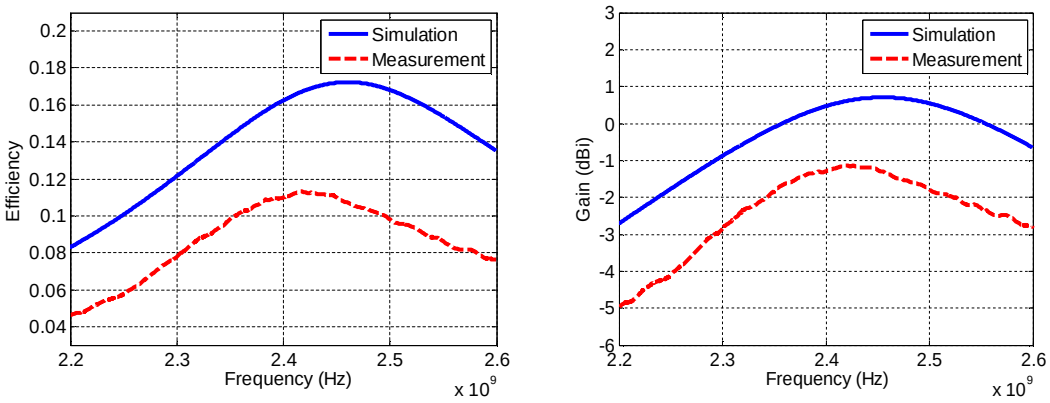

Figure 44. The measurment and simulation results of patch antenna for efficiency and gain.

The measurement setup for investigation the performance of system is represented in Fig. 45. A signal generator is used to power the patch antenna, and then the rectenna is placed near the reference antenna

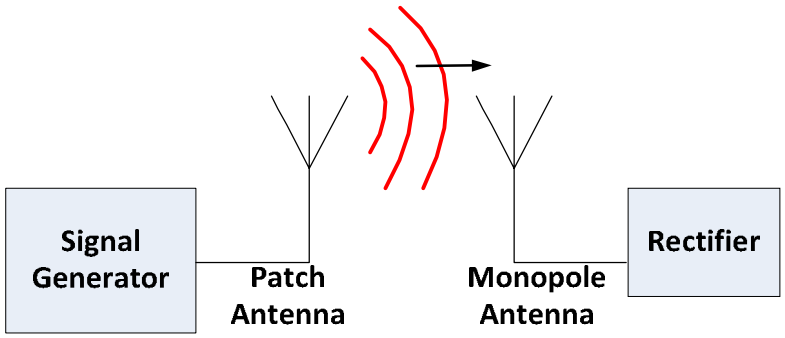

Figure 45. The measurment setup for investigating the performance of RF energy harvester.

The maximum received power by monopole antenna while the input power of signal generator is 20dBm, is measured by spectrum analyzer @ 2.4GHz. The maximum received power is around (-13_-12 dBm) if monopole antenna is located near patch antenna. The below table shows the measurement results of output voltage when monopole antenna is connected to rectifier and when rectifier is measured directly by signal generator.

Table 8. The output measurment result of RF energy harvester.

Input Power (dBm)	Output voltage rectifier without antenna(mV)	Output voltage of Rectifier with antenna(mV)
-13	4.1	4.3
-12	6.6	-
-11	11.4	-

Although there is a limitation in measurement, since more power cannot be transferred to the patch antenna, but the final results shows that the RF power harvester works. It shows 4.3mV at the output for -13dBm input power.

9. CONCLUSION

In this master thesis, the design and fabrication of RF energy harvester using Inkjet-printing technology on environmentally bulk cardboard substrate is investigated. For these purpose, different steps has been done. As first attempt, a single stage rectifier based on diode-based voltage doubler is simulated and implemented on cardboard. By using the input-output characteristics of diode, input RF signal is converted to DC voltage. The amount of output DC voltage depends on several parameters: number of stages, load and capacitors. In addition, after fabrication of rectifier, the input impedance matching circuit was added, in order to transfer the maximum available power to the rectifier. The matching circuit is a critical part of design, since the input impedance of rectifier is change the variation of the input power level. Hence, the circuit should be matched in all input power range.

A series capacitors and shunt inductors were used in matching circuit. As measurement result shows, the circuit is perfectly matched the desire power range. The output DC voltage was measured before and after adding matching circuit. For 5dBm input power at 2.4GHz, 1.12V is presented at the output of voltage doubler.

In the next Step, a monopole planar antenna was simulated and fabricated on cardboard by inkjet-printing technique. A planar monopole antenna was chosen for power harvesting as power source since its radiation pattern is omnidirectional in the H plane and the radiation pattern does not change with frequency. The antenna was measured by Satimo_Star lab. The measurement shows a good agreement with simulation.

Finally, in the last step, rectifier was connected to the antenna and placed near a patch antenna as power sources. The maximum measured power by Agilent E4407B Spectrum Analyzer, which is captured by monopole antenna near power source, is almost –13 dBm. Connecting the monopole antenna to the rectifier, directly, and placing it near the power source, provides a DC voltage in the millivolt range across a 10 kΩ load. This correlates with the results of rectifier.

10. PUBLICATIONS

- IEEE RFID Technology and Applications (RFID-TA) Conference-2014: Hossein Saghlatoon, Zahra Khonsari, Lauri Sydänheimo, Manos M. Tentzeris and Leena Ukkonen, “Inkjet-Printed GSM900 Band RF Power Harvester on Paper-Based Substrates”.

- IEEE Radio and Wireless Symposium (RWS)-2015: Zahra Khonsari, Toni Björninen, Manos M. Tentzeris and Leena Ukkonen,”2.4GHz Inkjet-Printed Rf Power Harvester on Bulk Cardboard Substrate” (submitted).

REFERENCES

[1] J. Tavares, N. Barroca, H. M. Saraiva, L. M., Borges, F. J. Velez, C. Loss, N. Borges Carvalho,"Spectrum opportunities for electromagnetic energy harvesting from 350 mhz to 3 ghz," In Medical Information and Communication Technology (ISMICT), 2013 7th International Symposium on (pp. 126-130). IEEE ,March 2013.

[2] C. K. Toh, "Maximum battery life routing to support ubiquitous mobile computing in wireless ad hoc networks," Communications Magazine, IEEE, 39(6), 138-147, 2001.

[3] S. Sudevalayam, P. Kulkarni, " Energy harvesting sensor nodes: Survey and implications," Communications Surveys & Tutorials, IEEE, 13(3), 443-461, 2011.

[4] W. R. Heinzelman, A. Chandrakasan, H. Balakrishnan," Energy-efficient communication protocol for wireless microsensor networks," In System Sciences, 2000. Proceedings of the 33rd Annual Hawaii International Conference on (pp. 10-pp). IEEE, January 2000.

[5] T. Pering, Y. Agarwal, R. Gupta, R. Want, "Coolspots: reducing the power consumption of wireless mobile devices with multiple radio interfaces," In Proceedings of the 4th international conference on Mobile systems, applications and services (pp. 220-232). ACM, June 2003.

[6] M. Armand, J. M. Tarascon, "Building better batteries," Nature, 451(7179), 652-657, 2008.

[7] M.Rastmanesh, "High Efficiency RF to DC Converter with Reduced Leakage Current for RFID Applications", Dalhousie University, Halifax, Nova Scotia, April 2013.

[8] Zahriladha Zakaria, Nur Aishah Zainuddin, Mohd Nor Husain, Mohamad Zoinol Abidin, "Current Developments of RF Energy Harvesting System for Wireless". Advances in information Sciences and Service Sciences (AISS).June 2013.

[9] K. K. A. Devi, N. M. Din, C. K. Chakrabarty,"Optimization of the Voltage Doubler Stages in an RF-DC Convertor Module for Energy Harvesting," Circuits & Systems, 3(3), 2012.

[10] HSMS-2850, "Surface Mount Zero Bias Schottky Detector Diodes." http://www.crystal-radio.eu/hsms285xdata.pdf

[11] HSMS-2820, "Surface Mount Zero Bias Schottky Detector Diodes."http://www.digchip.com/datasheets/parts/datasheet/021/HSMS-2820-pdf.php.

[12] Kraus, J.D. Fliesch, D.A. Electromagnetics with Applications. 5th Edition. The USA, McGraw-Hill. 1999.

[13] Pozar, D.M. Microwave Engineering. The USA, Addison-Wesley Publishing Company. 1990. 719 p.

[14] Kraus, J.D. Antennas for All Applications. 3rd Edition. The USA, McGraw-Hill. 2002. 921 p.

[15] Balanis, C.A. Antenna Theory Analysis and Design. 2nd Edition. The USA, John Wiley & Sons, Inc. 1997. 931 p.

[16] Stutzman, W.L. Thiele, G.A. Antenna Theory and Design. 2nd Edition. The USA, John Wiley & Sons, Inc. 1998. 643 p.

[17] Hon, K.K.B, Li, L. Hutchings, I.M. 2008. Direct Writing Technology-Advances and Developments. CIRP Annals-Manufacturing Technology 57, 2, p 601-620.

[18] Le, H.P. Progress and tend in inkjet printing proteins and hybrid cell-containing materials and structure. Jornal of Materials Chemistry , 18(2008) 47,PP.5717-5721.

[19] Harima Chemicals, Inc. NPS-JL Silver Nanoparticle Ink, NanoPaste Series, Metal Paste for Thin Film Formation [WWW].[Accessed on 20.4.2014]. Available at: http://www.harima.co.jp/en/products/pdf/16-17e.pdf

[20] H.Saghlatoon, ”Inljet-Printed Circuits on Fibrous Substrate for Enviermentally-Friendly RF Electronics Applications, “ April 2014.

[21] Katehi, P. B, and N.G. Alexopolos, “on the Effect of Substrate Thickness and Permittivity on Printed Circuit Dipoles Properties” , IEEE Trans. on Antenna and Propagartion, Vol. AP-31, 1983, PP.34-38.

[22] James, J. R, P.S Hall, and C. Wood, “Microstrip Antennas: Theory and Design, Peter Peregrinus, London, UK, 1989.

[23]James, J. R, P.S Hall, “Handbook of Microstrip Antennas” , Peregrinus, London, UK, 1989.

[24]Constantine. A. Balanis, “Antenna Theory: Analysis and Design”, 3rd edition, John Wiley & Sons, Inc. New Jersey 2005.ISBN: 0-41-66782-X.

[25]Dubost, G, “Flat Radiating Dipoles and Applications to Arrays”, Research Studies Press, New York, 1981.

[26]Oliner, A. A, “The Radiation Conductance of a series Slot in Strip Transmission Line”, IRE National Conv. Rec, Vol, 2, Part8, 1954.

[27]Rao, J. S and B. N. Das, “Impedance of OFF-Centered Strip Line Fed Series Slot”, IEEE Trans. on Antennas and Propagations, Vol. 1988.

[28]Bahl. I.J and P. Bhartia, “Microstrip Antenna Design Handbook”, Artech House, Dedham, MA, 1980.

[29]Kumar. G and K. P. Ray, “Broad Band Microstrip Antennas” ,Artech House. Boston. London. 2003.

[30]H. Saghlatoon, L. Sydänheimo, L. Ukkonen, M. M. Tentzeris, “Optimization of inkjet printing of patch antennas on low-cost fibrous substrates,” IEEE Antennas Wireless Propag. Lett., vol. 13, no. 1, pp. 915-918, Dec. 2014.